AUSTRALIAN JOURNAL OF BASIC AND APPLIED SCIENCES

ISSN:1991-8178 EISSN: 2309-8414
Journal home page: www.ajbasweb.com

A Novel Three Degree of Freedom Stewart-like Platform for Testing Humanoid Postural Capabilities

Abdallah Bader, Alaa EddinAlsharawi,Mahmoud Saeed, Karim Tahboub

Palestine Polytechnic University, Mechanical engineering department, Faculty of engineering, Hebron, Palestine.

Address For Correspondence:
Abdallah Bader, Palestine Polytechnic University, Mechanical engineering department, Faculty of engineering. Box.198. Hebron. Palestine.

ARTICLE INFO

Article history:
Received 18 January 2017
Accepted 28 March 2017
Available online 1 May 2017

Keywords:
Humanoids, Balance, Postural, Sagittal, Stewart platform, Parallel manipulator.

ABSTRACT

In this paper, a novel design of a Stewart-like platform is introduced with the purpose of testing humanoids postural capabilities. It performs three motions including surge (forward-backward), heave (up-down), and pitch (tilting). The suggested novel design is inspired from Stewart platform, a kind of parallel manipulator, distinguished for its high stability, and rigidity, but a narrower workspace compared to serial manipulators. Stewart platform provides six degrees of freedom, which are more kinds of motions than needed for testing humanoids balance. For this, Stewart platform is optimized to perform required motions to test humanoids balance of surge, heave, and pitch, by reducing the numbers of actuators from six to four, and re-configuring joints and links connecting the platform to its fixed base. While four actuators are sufficient for three degrees of freedom, 4th actuator was added for wider stability range, which adds the possibility for 4th motion of rolling. Mathematical analyses are conducted for the suggested novel design including kinematics, Jacobians, and dynamic modeling using both Lagrange formulation and Newton Euler methods, those analysesare based on the side view projection of the platform. Different control techniques were considered including model based controller, and independent joint controller. MATLAB Simulink was the software environment simulation has been conducted in, where S-function tool is used to replace the plant through its derived dynamic equations for the purpose of testing model based controller. CATIA software was used to 3D model the new design, and to manipulate its parts observing its motion. CATIA was also used to conduct structural analysis of the platform.A prototype has been built and controlled to demonstrate the new design performing surge, heave, and pitch motions.Prototype has shown high rigidity, and high stability. The new design can be considered for various types of applications other than testing humanoids balance, including simulators,and machining technologies.

INTRODUCTION

This paper describes a novel design ofa Stewart-like platform, including design structure analysis, kinematics derivation, controller design, simulation results, and experimental results extracted from a built prototype. Where the need for such a design was inspired from testing humanoids postural stability (Tahboub 2011). The new design introduced in this paper is based on Figure1, which shows side view projection of the suggested novel design. Where links with variating lenghts can make the platform perform surge, heave, & pitch motion. While some designs can perform surge, heave, and pitch motions such as (Harda and Liu 2013), Stewart platform holds much rigidity and stability.

To Cite This Article: Abdallah Bader, Alaa EddinAlsharawi,Mahmoud Saeed, Karim Tahboub., A Novel Three Degree of Freedom Stewart-like Platform for Testing Humanoid Postural Capabilities. ***Aust. J. Basic & Appl. Sci.,*** *11(5): 113-125, 2017*

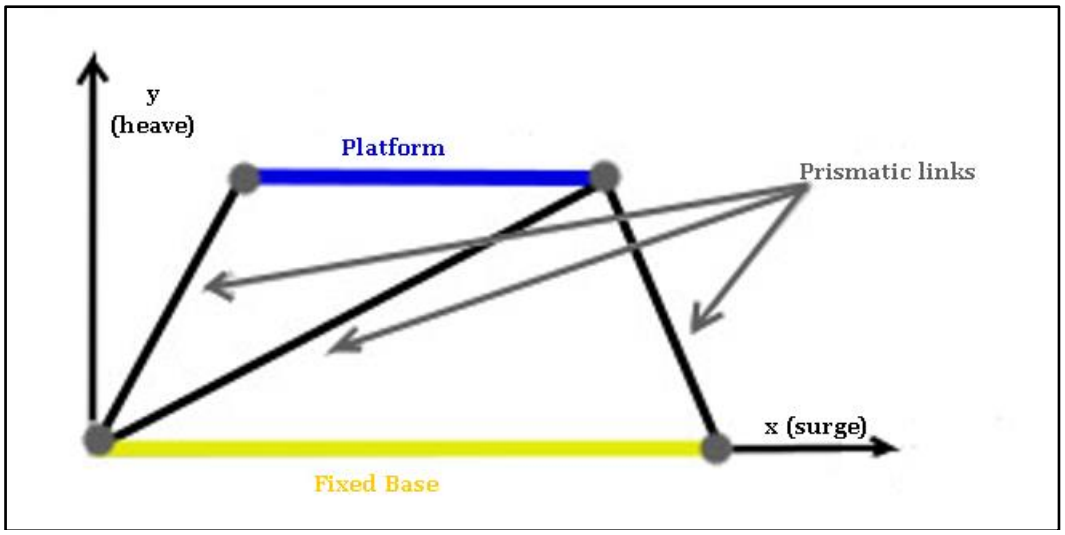

Fig. 1: Side view projection of 3DOF Stewart-like platform

To utilize the design suggested in Figure 1, Stewart platform was considered. Figure 2(Derek 2015) shows different types of Stewart platform, which are classified with regards to the number of connecting points on both platform and fixed base. Stewart platform type 3-3 was looked upon to satisfy the side view projection suggested in Figure 1, with equal lengths considerations demonstrated in Figure 3.(Staicu 2009) provides kinematics and dynamic description of 3-3 type.

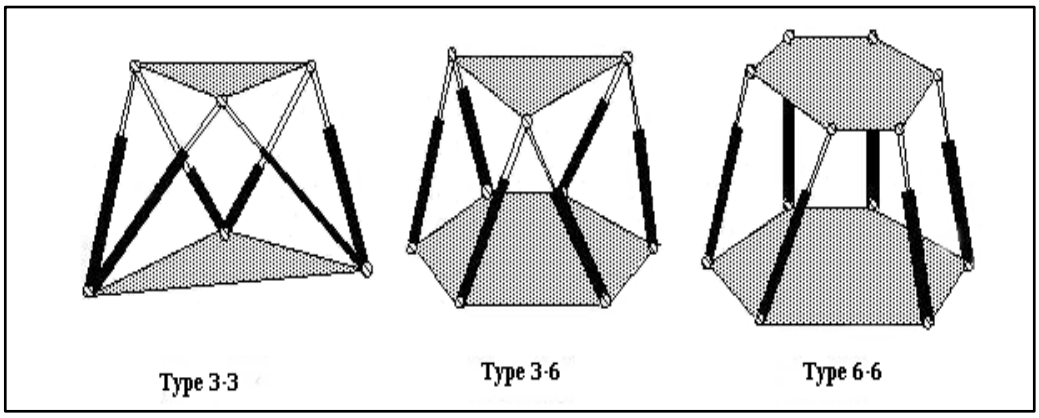

Fig. 2: Stewart like platform types, with types n-m, where n refers to number of joints connecting the upper platform, and m refers to number of joints connecting the base (Derek 2015).

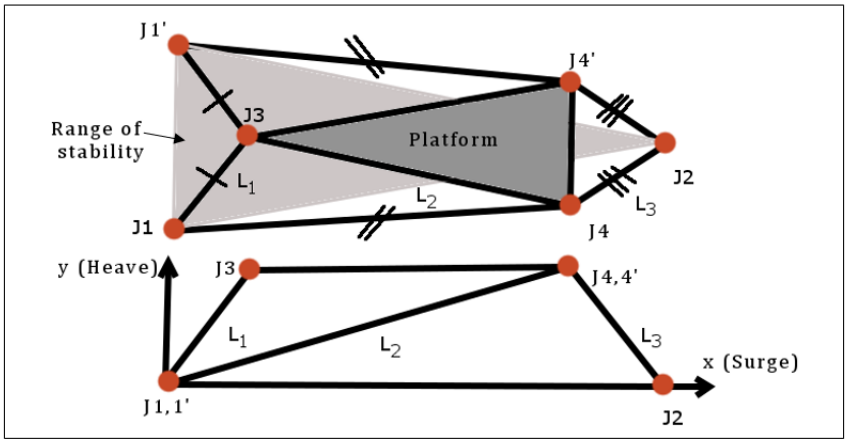

Fig. 3: Stewart platform type 3-3 with equal parallel lengths considered to achieve three motions based on the demonstrated side view projection- including surge, heave, and pitch, where J denotes joint, and L denotes link.

Australian Journal of Basic and Applied Sciences, 11(5) April 2017, Pages: 113-125

New Design:

For only 3DOF's are required for postural capabilities testing, which are surge, pitch, and heave, number of actuators shown in Figure 3 are to be reduced. Figure 4 shows the final design of the platform. This design was chosen among other designs satisfying the side view projection shown in Figure 1. This design provides a wide range of stability andsuitable workspace.

Figure 4 shows top-side view projection of the new design. This design provides three motions including surge, heave, and pitch, when considering L_3, and L'_3 to be of same length. Also this design could provide 4th kind of motion which is rolling when lengths of L_3 and $L'_3$are not equal.

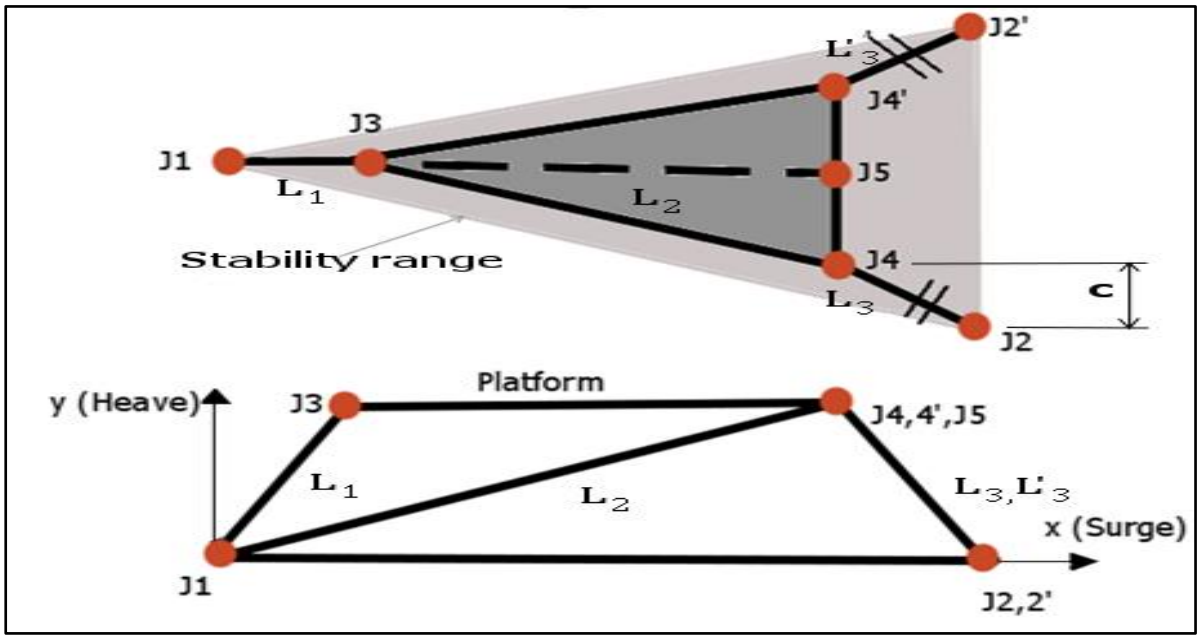

Fig. 4: 3DOF Stewart-like platform new design concept, where J denotes joint, L denotes links.

3D Model Realization:

Figure 5 represents the 3D model of the new platform design, Where $L_1, L_2, and\ L_3$ variates through active prismatic joints.

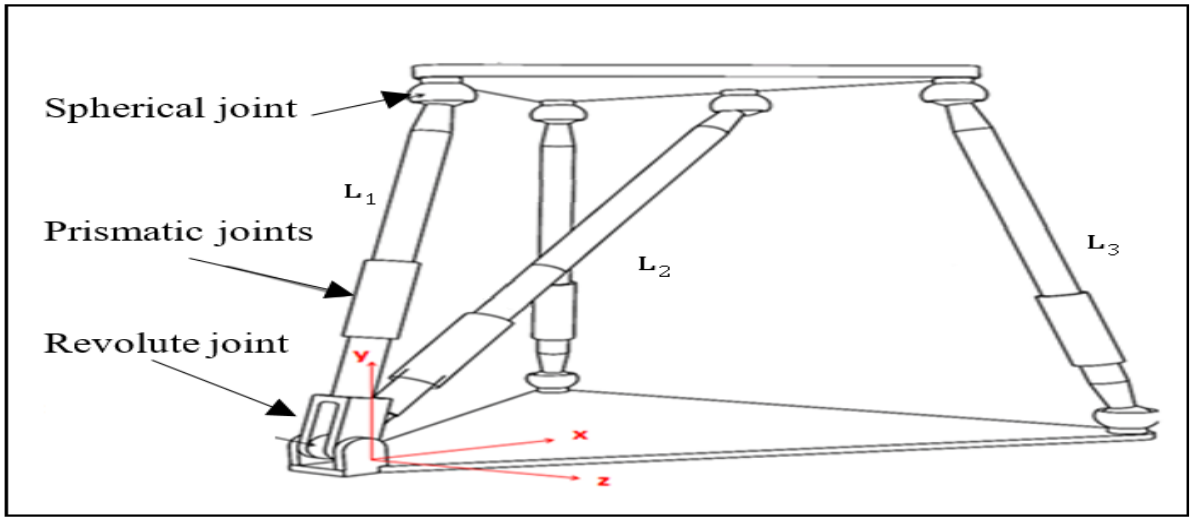

Fig. 5: 3D model concept of Stewart-like platform new design where L denotes link.

Materials and Dimensions:

Platform and connecting links were chosen to be made from aluminum since it is relatively light, and has a high strength of 70 $[MPa]$. Platform was designed with height of roughly 90 $[cm]$, having the square platform

of $50x50$ $[cm]$ where humanoid is expected to stand on with ease. Dimensions of the fixed triangle base are 80 $[cm]$ base length and 80 $[cm]$height. Both platform and base are of thickness of 5 $[mm]$.Where overall length$L_1, L_2, and\ L_3$,are$85, 100, 87$ $[cm]$ respectively, with motors at stroke of 10 $[cm]$, where linear motors has a full stroke of 20 $[cm]$, connecting links has $2.5x2.5$ $[cm^2]$ cross section. Greatest use of variating actuators strokes has been achieved. Figure 6 represents an overview of the actual 3D model.

Structural Analysis:

In order to build prototype; structural analysis has been done using CATIA shown in Figure 6. With an allowable stress of roughly $70Mpa$ of aluminum von misses stresses shown in Figure 6 were deemed applicable, having a maximum equivalent stress of $1.05MPa$ acting upon platform.Where structural load of 500[N] where applied upon platform.

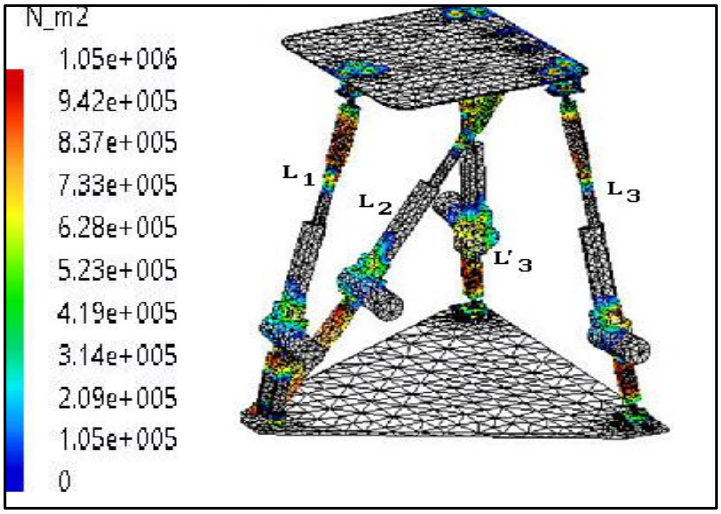

Fig. 6: Von missesstresses acting on platform**.**

Geometrical Constraints:

Maximum angle of 30°coming from spherical joints was also considered not to be overreached throughout workspace. 3D model was manipulated through CATIA to check forcollision between parts.

MATERIALS AND METHODS

Forward Kinematics:

Considering the Figure 7 showing side view projection of platform with arbitrary platform location of $(x, y, and\ \theta)$, which can be determined by Lengths $L1$, $L2$, and $L3xy$ through the following forward kinematics. Through equations (1-23). Where d is the platform length, and p is the base length.

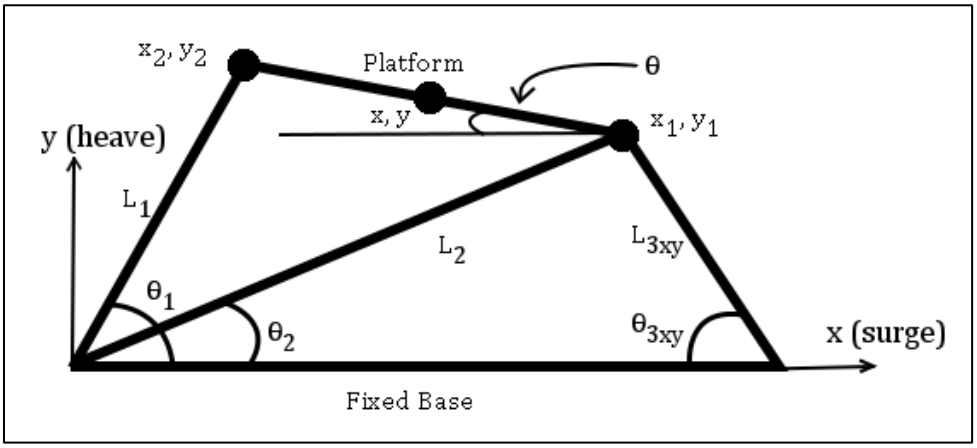

Fig. 7: Side view projection of platform with arbitrary position of platform center x, y, and θ.

Australian Journal of Basic and Applied Sciences, 11(5) April 2017, Pages: 113-125

$$L_3^2 = L_{3xy}^2 + c^2 \quad (1)$$

Where constant c is represented on Figure 4, thus L_{3xy} can be calculated as follows

$$L_{3xy} = \sqrt{L3^2 - c^2} \quad (2)$$

For upper right corner, position can be calculated as

$$x_1 = L_2 \cos\theta_2 \quad (3)$$

$$y_1 = L_2 \sin\theta_2 \quad (4)$$

For upper left corner, position can be calculated as

$$x_2 = L_1 \cos(\theta_1) \quad (5)$$

$$y_2 = L_1 \sin(\theta_1) \quad (6)$$

For θ_{12}, which is defined as

$$\theta_{12} = \theta_1 - \theta_2 \quad (7)$$

The following trigonometric equations applies

$$\cos\theta_{12} = \frac{L_1^2 + L_2^2 - d^2}{2L_1L_2} \quad (8)$$

And using trigonometric identity

$$\sin\theta_{12} = \sqrt{1 - \cos^2\theta_{12}} \quad (9)$$

Similarly, using cosine law for θ_2

$$\cos\theta_2 = \frac{p^2 + L_2^2 - L_{3xy}^2}{2L_2 \cdot p} \quad (10)$$

Using trigonometric identity

$$\sin\theta_2 = \sqrt{1 - \cos^2\theta_2} \quad (11)$$

To find upper right x_1 coordinate corner we substitute the value of $\cos\theta_2$ into x_1 equation

$$x_1 = \frac{p^2 + L_2^2 - L_{3xy}^2}{2 \cdot p} \quad (12)$$

To find upper right y_1 coordinate corner we substitute the value of $\sin\theta_2$ into y_1 equation

$$y_1 = L_2\sqrt{1 - \left(\frac{p^2 + L_2^2 - L_{3xy}^2}{2 \cdot L_2 p}\right)^2} \quad (13)$$

To find upper left x_2 coordinate corner position

$$x_2 = L_1(\cos\theta_{12}\cos\theta_2 - \sin\theta_{12}\sin\theta_2) \quad (14)$$

By substituting the values of $sines$ and $cosines$ of θ_2, and θ_{12} into x_2

$$x_2 = L_1\left(\left(\frac{p^2 + L_2^2 - L_{3xy}^2}{2 \cdot L_2 \cdot p}\right) \cdot \left(\frac{L_1^2 + L_2^2 - d^2}{2L_1L_2}\right) - \sqrt{1 - \left(\frac{p^2 + L_2^2 - L_{3xy}^2}{2 \cdot L_2 \cdot p}\right)^2} \cdot \sqrt{1 - \left(\frac{L_1^2 + L_2^2 - d^2}{2L_1L_2}\right)^2}\right) \quad (15)$$

To find upper left y_2 coordinate corner position

$$y_2 = L_1(\sin\theta_{12}\cos\theta_2 + \cos\theta_{12}\sin\theta_2) \quad (16)$$

By substituting the values of sines and cosines

$$y_2 = L_1\left(\sqrt{1 - \left(\frac{p^2 + L_2^2 - L_{3xy}^2}{2 \cdot L_2 \cdot p}\right)^2} * \left(\frac{L_1^2 + L_2^2 - d^2}{2L_1L_2}\right) + \left(\frac{p^2 + L_2^2 - L_{xy3}^2}{2 \cdot L_2 \cdot p}\right) * \sqrt{1 - \left(\frac{L_1^2 + L_2^2 - d^2}{2L_1L_2}\right)^2}\right) \quad (17)$$

To find platform position represented through (x, y) first x coordinate is found as follows

$$x = \frac{x_1 + x_2}{2} \quad (18)$$

Substituting the value of x1 and x2

$$x = \frac{p^2 + L_2^2 - L_{3xy}^2}{4 \cdot p} + \frac{L_1}{2}\left(\frac{p^2 + L_2^2 - L_{3xy}^2}{2 \cdot L_2 \cdot p}\right) \cdot \left(\frac{L_1^2 + L_2^2 - d^2}{2L_1L_2}\right) - \frac{L_1}{2}\sqrt{1 - \left(\frac{p^2 + L_2^2 - L_{3xy}^2}{2 \cdot L_2 \cdot p}\right)^2} \cdot \sqrt{1 - \left(\frac{L_1^2 + L_2^2 - d^2}{2L_1L_2}\right)^2} \quad (19)$$

To find coordinate y

$$y = \frac{y_1 + y_2}{2} \quad (20)$$

By substituting the value of y1, and y2

$$\boldsymbol{y} = \frac{L_2}{2}\sqrt{1 - \left(\frac{p^2 + L_2^2 - L_{3xy}^2}{2 \cdot L_2 \cdot p}\right)^2} + \frac{L_1}{2}\sqrt{1 - \left(\frac{p^2 + L_2^2 - L_{3xy}^2}{2 \cdot L_2 \cdot p}\right)^2} * \left(\frac{L_1^2 + L_2^2 - d^2}{2L_1L_2}\right) + \frac{L_1}{2}\left(\frac{p^2 + L_2^2 - L_{3xy}^2}{2 \cdot L_2 \cdot p}\right) * \sqrt{1 - \left(\frac{L_1^2 + L_2^2 - d^2}{2L_1L_2}\right)^2} \quad (21)$$

Now finally to calculate the tilting angle the following trigonometry is used.

$$\tan\theta = \frac{y_1 - y_2}{x_1 - x_2} \quad (22)$$

By substituting the values of $x1, y1, x2, and\ y2$

$$\tan\theta = \frac{L_2\sqrt{1 - \left(\frac{p^2+L_2^2-L_{3xy}^2}{2 \cdot L_2 p}\right)^2} - L1\sqrt{1 - \left(\frac{p^2+L_2^2-L_{3xy}^2}{2 \cdot L_2 p}\right)^2} * \left(\frac{L_1^2+L_2^2-d^2}{2L_1L_2}\right) - L1\left(\frac{p^2+L_2^2-L_{3xy}^2}{2 \cdot L_2 p}\right) * \sqrt{1 - \left(\frac{L_1^2+L_2^2-d^2}{2L_1L_2}\right)^2}}{\frac{p^2+L_2^2-L_{3xy}^2}{2 \cdot p} - L1\left(\frac{p^2+L_2^2-L_{xy3}^2}{2 \cdot L_2 p}\right) \cdot \left(\frac{L_1^2+L_2^2-d^2}{2L_1L_2}\right) + L1\sqrt{1 - \left(\frac{p^2+L_2^2-L_{3xy}^2}{2 \cdot L_2 p}\right)^2} \cdot \sqrt{1 - \left(\frac{L_1^2+L_2^2-d^2}{2L_1L_2}\right)^2}} \quad (23)$$

To calculate θ, we take $arc\ tan$ of eq. 23.

Inverse Kinematics:

Considering Figure 6. Inverse kinematics can be found through equations (24-35). To find lengths $L_1, L_2, and\ L_3$, each upper left, and right corner's position is to be specified. Then lengths can be found through Pythagorean theorem.Where d is the platform length, and p is the base length.

The location of the left upper joint of the platform in x-coordinate

$$x_2 = x - (d\ /\ 2)\cos\theta \quad (24)$$

Similarly, the location of this joint in y-direction

$$y_2 = y + (d/2)\sin\theta \quad (25)$$

The location of the right upper joint of the platform in x-coordinate

$$x_1 = x + (d|2)\cos\theta \quad (26)$$

Similarly, the location of the joint in y-direction

$$y_1 = y - (d/2)\sin\theta \quad (27)$$

Now when the joint locations are known according to x-y plane the lengths of the links will be found. The length of Link1 will determine from left upper joint coordinates $x_2$and y_2

$$L_1 = \sqrt{x_2^2 + y_2^2} \quad (28)$$

By submitting terms of$x_2$and y_2 into the eq. and simplifying.

$$L_1 = \sqrt{x^2 + y^2 + yd.sin\theta - xd.cos\theta + \frac{d^2}{4}} \quad (29)$$

Having known the position of the right upper joint coordinates $x_1$and y_1 link2 can be calculated as follows

$$L_2 = \sqrt{x_1^2 + y_1^2} \quad (30)$$

By submitting the terms of $x_1$and $y_1$into equation and simplifying.

$$L_2 = \sqrt{x^2 + y^2 - yd.sin\theta + xd.cos\theta + \frac{d^2}{4}} \quad (31)$$

The length of the projection of link3 in $x - y$ plane

$$L_{3xy} = \sqrt{(p - x_1)^2 + y_1^2} \quad (32)$$

By substituting terms of $x_1$and y_1

$$L_{3xy} = \sqrt{p^2 - 2px - pd.cos\theta + x^2 + y^2 - yd.sin\theta + xd.cos\theta + \frac{d^2}{4}} \quad (33)$$

Length $L3$ is determined as follows

$$L_3 = \sqrt{{L_{3xy}}^2 + c^2} \quad (34)$$

By substituting terms into equation

$$L_3 = \sqrt{p^2 - 2px - pd.cos\theta + x^2 + y^2 - yd.sin\theta + xd.cos\theta + \frac{d^2}{4} + c^2} \quad (35)$$

Jacobian and Jacobian Inverse Matrices:

Jacobian matrix of the system proposed presents the relationship between $\dot{x}$, $\dot{y}$, and $\dot{\theta}$, with $\dot{L}_1$, $\dot{L}_2$, and $\dot{L}_3$, i.e. given $\dot{L}_1$, $\dot{L}_2$, and $\dot{L}_3$, we can find $\dot{x}$, $\dot{y}$, and $\dot{\theta}$. This was done through deriving eq. $(19, 21, 32)$.

Jacobian inverse matrix of the system proposed presents the relationship between $\dot{x}$, $\dot{y}$, and $\dot{\theta}$, with $\dot{L}_1$, $\dot{L}_2$, and $\dot{L}_3$, i.e. given$\dot{x}$, $\dot{y}$, and $\dot{\theta}$, we can find$\dot{L}_1$, $\dot{L}_2$, and $\dot{L}_3$. This was done through deriving eq. $(29, 31, 35)$.

Both matrices and derivations shall be provided upon request to the corresponding email.

Dynamic Model Using Lagrange Formulation:

Lagrange formulation is used to derive the dynamic model of the side projection of the platform shown in Figure 8. Where actuating links are considered massless, and joints friction is not taken into consideration.

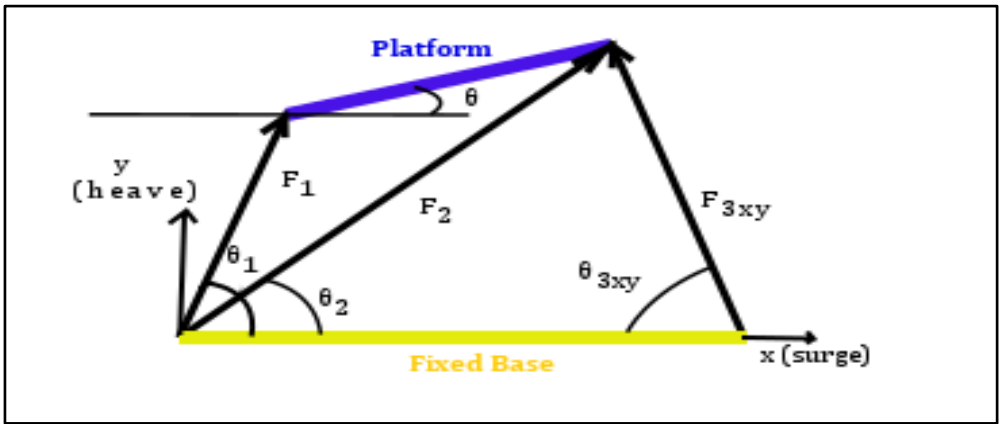

Fig. 8: Side view projection of acting forces upon platform

Considering $q = [x, y, \theta]^T$and τas the corresponding generalized coordinates and generalized forces, respectively, the general classical equation of motion can be obtained from the following Lagrange formulation.

$$\frac{d}{dt}\left(\frac{\partial L}{\partial \dot{q}}\right) - \frac{\partial L}{\partial q} = \tau \quad (36)$$

Where L the Lagrange function is considered as

$$L = T - U \quad (37)$$

Where T, and U are kinetic and potential energies respectively. Taking into count that humanoid center of mass is on a vertical coincidence with platform center, and assuming links are massless, kinetic energy is

considered as follows. Where m_h, m_p, I_h, and I_p, represents platform, and humanoid mass, and inertias. Where humanoids center of gravity is assumed on a vertical coincidence with platforms center at all times

$$\mathrm{T} = \frac{1}{2}(m_p + m_h)v_x^2 + \frac{1}{2}(m_p + m_h)v_y^2 + \frac{1}{2}(I_p + I_h)\omega^2 \quad (38)$$

And potential energy is considered as follows

$$\mathrm{U} = (m_p + m_h) * g * y \quad (39)$$

Applying Lagrange formulation in each x, y, θ direction; starting with x direction the Lagrange function is considered as follows

$$L = \frac{1}{2}(m_p + m_h)v_x^2 \quad (40)$$

Lagrange formulation in x direction is considered as follows

$$\frac{d}{dt}\left(\frac{\partial L}{\partial \dot{x}}\right) - \frac{\partial L}{\partial x} = \Sigma F_x \quad (41)$$

Where, the velocity in x direction

$$v_x = \dot{x} \quad (42)$$

And

$$\frac{\partial L}{\partial \dot{x}} = (m_p + m_h)\dot{x} \quad (43)$$

But

$$\frac{\partial L}{\partial x} = 0 \quad (44)$$

Lagrange formulation left term is simplified as follows

$$\frac{d}{dt}\left(\frac{\partial L}{\partial \dot{x}}\right) - \frac{\partial L}{\partial x} = \frac{d}{dt}\left((m_p + m_h)\dot{x}\right) = (m_p + m_h)\ddot{x} \quad (45)$$

$$\Sigma F_x = F_1 cos\theta_1 + F_2 \cos\theta_2 - 2F_3 cos\theta_{3x} \quad (46)$$

Where $\theta_1, and\ \theta_2$are illustrated on Figure 8, andθ_{3x} is the angle between $F3$ line of action and x-axis Finally, Lagrange formulation final form in x coordinate is given as follows

$$(m_p + m_h)\ddot{x} = F_1 cos\theta_1 + F_2 \cos\theta_2 - 2F_3 cos\theta_{3x} \quad (47)$$

In y-axis, Lagrange function is considered as follows.

$$L = \frac{1}{2}(m_p + m_h)V_y^2 - (m_p + m_h) * \mathrm{g} * \mathrm{y} \quad (48)$$

Lagrange formulation in y direction is considered as follows

$$\frac{d}{dt}\left(\frac{\partial L}{\partial \dot{y}}\right) - \frac{\partial L}{\partial y} = \Sigma F_y \quad (49)$$

Where the velocity in y direction

$$\dot{y} = V_y \quad (50)$$

And,

$$\frac{\partial L}{\partial \dot{y}} = (m_p + m_h)\dot{y} \quad (51)$$

Considering that

$$\frac{\partial L}{\partial y} = -(m_p + m_h) * \mathrm{g} \quad (52)$$

Lagrange formulation left term is simplified as

$$\frac{d}{dt}\left(\frac{\partial L}{\partial \dot{y}}\right)\frac{\partial L}{\partial y} = (m_p + m_h)\ddot{y} + (m_p + m_h) * \mathrm{g} \quad (53)$$

Considering the sum of acting forces in $y$direction as follows

$$\Sigma F_y = F_1 * \sin\theta_1 + F_2 * \sin\theta_2 + 2F_3 \cos\theta_{3y} \quad (54)$$

Where $\theta 1, and\ \theta 2$ are illustrated on Figure 8, and $\theta 3y$ is the angle between F3 line of action and y-axisFinally, Lagrange final form is

$$(m_p + m_h)\ddot{y} + (m_p + m_h) * \mathrm{g} = F_2 * \sin\theta_2 + F_1 * \sin\theta_1 + 2F_3 \cos\theta_{3y} \quad (55)$$

In θ-direction, Lagrange function is considered as follows

$$L = \frac{1}{2}(I_p + I_h)\omega^2 \quad (56)$$

Where velocity in θ direction is taken as

$$\omega = \dot{\theta} \tag{57}$$

And,

$$\frac{\partial L}{\partial \dot{\theta}} = (I_p + I_h)\dot{\theta} \tag{58}$$

Considering that

$$\frac{\partial L}{\partial \theta} = 0 \tag{59}$$

Lagrange formulation left term can be expressed as follows

$$\frac{d}{dt}\left(\frac{\partial L}{\partial \dot{\theta}}\right) - \frac{\partial L}{\partial \theta} = (I_p + I_h) \tag{60}$$

Considering the sum of acting moment around platform center in $\boldsymbol{\theta}$direction as follows

$$\Sigma M_c = \mathrm{r} * (-F_1 * \sin(\theta_1 - \theta) + F_2 * \sin(\theta_2 - \theta) + 2F_{3xy} * \sin(\theta + \theta_{3xy})) \tag{61}$$

Where F_{3xy} represents side view projection of force F3 shown in Figure 8.

$$F_{3xy} = F_3\sqrt{cos^2\theta 3x + cos^2\theta 3y} \tag{62}$$

Finally, Lagrange formulation in θ direction becomes

$$(I_p + I_h)\ddot{\theta} = \mathrm{r}\left(-F_1 \sin(\theta_1 - \theta) + F_2 \sin(\theta_2 - \theta) + 2F_3\sqrt{cos^2\theta_{3x} + cos^2\theta_{3y}}\ \sin(\theta + \theta_{3xy})\right) \tag{63}$$

Dynamic Model Using Newton Euler Method:

Sum of forces in x direction

$$\Sigma F_x = (m_p + m_h)\ddot{x} \tag{64}$$

Substituting sum of forces acting in x direction yeilds,

$$(m_p + m_h)\ddot{x} = F_1 cos\theta_1 + F_2 \cos\theta_2 - 2F_3 \cos\theta_{3x} \tag{65}$$

Sum of forces in y direction

$$\Sigma F_y = (m_p + m_h)\ddot{y} \tag{66}$$

Substituting sum of forces acting in y direction yeilds,

$$(m_p + m_h)\ddot{y} + (m_p + m_h) * \mathrm{g} = F_2 * \sin\theta_2 + F_1 * \sin\theta_1 + 2F_3\cos\theta_{3y} \tag{67}$$

Sum of forces in θ direction

$$\Sigma M_C = (I_p + I_h)\ddot{\theta} \tag{68}$$

Substituting sum of acting moments in θ direction yields,

$$(I_p + I_h)\ddot{\theta} = \mathrm{r}\left(-F_1 \sin(\theta_1 - \theta) + F_2 \sin(\theta_2 - \theta) + 2F_3\sqrt{cos^2\theta_{3x} + cos^2\theta_{3y}}\sin(\theta + \theta_3)\right) \tag{69}$$

We conclude that Newton method gives same modeling result as Lagrangeformulation. Note that dynamic model of the platform disregards the mass of actuating links and the friction of moving joints.

Model Based Controller:

Having the platform at an arbitrary position, provided that platform is to move to a desired set position, required joint forces $(F_1, F_2, and\ F_3)$are to be applied upon the platform.In the dynamic model, Nonlinearities presents on forces side, thus we can use linear state space model to design controller which provides Cartesian forces of $(F_x, F_y, and\ M_z)$ required to move the platform, then using Jacobian transpose we can compensate nonlinearities by online calculating joint forces (Spong and Vidyasager 1989).This is demonstrated in Figure 9.

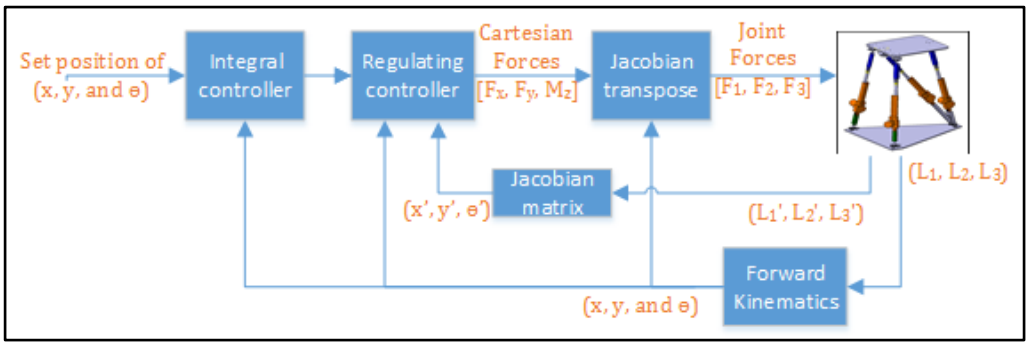

Fig. 9: Block diagram of tracking control using Jacobian transpose to compensate for nonlinearities.

Using state space model. Dynamics of the system is represented as follows.

$$\dot{\bar{x}} = A\bar{x} + B\bar{u} \quad (70)$$
$$\bar{y} = C\bar{x} + D\bar{u} \quad (71)$$

Where $\bar{x}$ is the state vector, that is equal to $\bar{x} = [x \quad \dot{x} \quad y\dot{y} \quad \theta \quad \dot{\theta}]'$, where x represents surge motion, y represents heave motion, and θ represents tilting angle in the sagittal plane, $\dot{\bar{x}}$ is the state derivatives vector, $\bar{y}$ is the output vector, $\bar{u}$is the input vector.

A is the system matrix, B is the input matrix, C is the output matrix, and D is the feedforward matrix, in our case system model does not have a direct feedforward so matrix D is a zero matrix. This could be represented as follows.

$$\dot{\bar{x}} = \begin{bmatrix} 0 & 1 & 0 & 0 & 0 & 0 \\ 0 & 0 & 0 & 0 & 0 & 0 \\ 0 & 0 & 0 & 1 & 0 & 0 \\ 0 & 0 & 0 & 0 & 0 & 0 \\ 0 & 0 & 0 & 0 & 0 & 1 \\ 0 & 0 & 0 & 0 & 0 & 0 \end{bmatrix} \bar{x} + \begin{bmatrix} 0 & 0 & 0 \\ 1/(m_p + m_h) & 0 & 0 \\ 0 & 0 & 0 \\ 0 & 1/(m_p + m_h) & 0 \\ 0 & 0 & 0 \\ 0 & 0 & 1/(I_h + Ip) \end{bmatrix} \bar{u} \quad (72)$$

$$\bar{y} = \begin{bmatrix} 1 & 0 & 0 & 0 & 0 & 0 \\ 0 & 0 & 1 & 0 & 0 & 0 \\ 0 & 0 & 0 & 0 & 1 & 0 \end{bmatrix} \bar{x} \quad (73)$$

Where m_h is humanoids mass,m_p is platform mass, $I_h$is humanoid's inertia, Ip is platforms inertia.Tracking controller was designed with the following control law represented in Figure 8. Where

$$\bar{u} = -K * \bar{x} + K_i * \bar{e} \quad (74)$$

Controller was built with the following specifications. Aworking frequency of no less than 1hz over 6° of tilting, and 10 cm of surge, and heave. And a settling time of at most $Ts = 1$[sec],the following desired poles locations are set by trial as

$$Poles = [-6.3 \ -6.4 \ -6.5 \ -6.8 \ -7 \ -7.1 \ -7.2 \ -7.3 \ -7.4] \quad (72)$$

Where integral gain K_i, and regulator gain K can be found through pole placement method counted for the extended system after adding the new gains. This means we can represent the overall system with extended system matrix Ae, and an extended input matrix Be. MATLAB was used to find the controller gains through finding gains Ke of the extended system as follows.

$$\gg Ke = place(Ae, Be, Pe)$$
$$\gg K = Ke(:,1:6)$$
$$\gg Ki = -Ke(:,7:9)$$

Where the following results were obtained

$$Ki = 1.0e+03 * \begin{bmatrix} 1.1294 & -0.0033 & -0.0394 \\ -0.0142 & 1.1463 & 0.0077 \\ -0.0009 & 0.0007 & 0.0251 \end{bmatrix} \quad (73)$$

$$K = \begin{bmatrix} 494.8621 & 72.1462 & -0.7181 & -0.0357 & -11.5286 & -0.8420 \\ -3.9605 & -0.2764 & 499.4951 & 72.4631 & 2.2697 & 0.1671 \\ -0.2488 & -0.0181 & 0.2134 & 0.0155 & 10.9659 & 1.5926 \end{bmatrix} \quad (74)$$

Controller has been tested in a MATLAB Simulink software environment with the same layout represented in Figure 9, where the plant has been represented through its nonlinear dynamic model, using S-function tool.

Australian Journal of Basic and Applied Sciences, 11(5) April 2017, Pages: 113-125

Independent Joint Controller:

With independent joint controller each individual motor is position controlled to the desired length of stroke. Where length of stroke is measured through encoders. Figure 10 shows how independent joint controller is carried out.

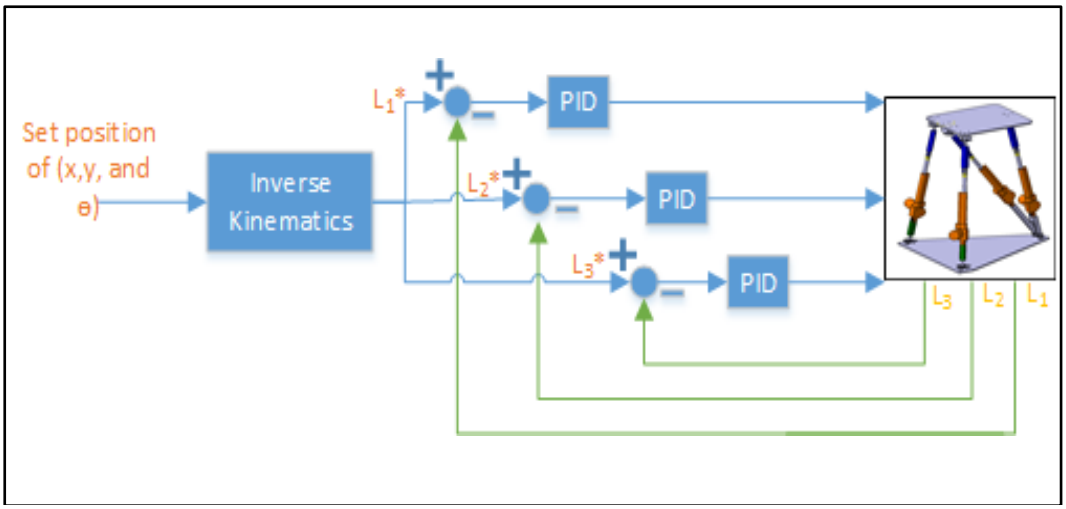

Fig. 10: Independent joint controller block diagram where * denotes desired value.

Experimental Setup:

Control was done through MATLAB Simulink using Arduino chip as control processor. Control blocks were built among Simulink. Input and output blocks of actual Arduino pins where used to receive and deliver position and control signals respectively. Independent join controller was implemented experimentally, rather than model based controller for there is no need for special motors that outputs a specific amount of force as required.

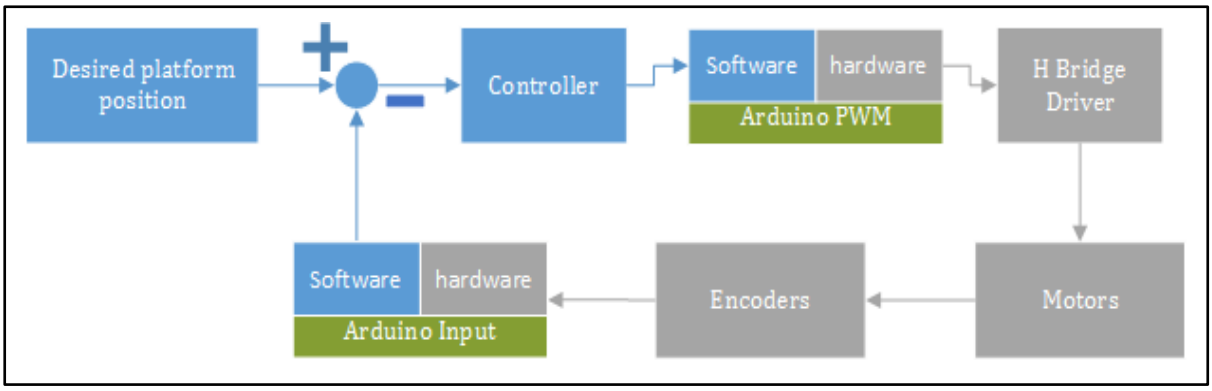

Fig. 11: Block diagram of implementing controller using Arduino

Block diagram shows how control was implemented. Grey blocks represents actual hardware, while blue ones represent software done in Simulink. Arduino blocks represents the connecting link between the two; while Arduino input and output software blocks are used to acquire and output signals, actual hardware chip is to connect actuators and encoders to the software part.

Results:

A desired step input was applied to the platform, the both results, experimental and simulation were obtained by MATLAB Simulink. Responses of surge, heave, and pitch motion are taken through encoders readings having it transformed to final positions using kinematics. The simulation and experiment result for the same input show how efficient the model is.

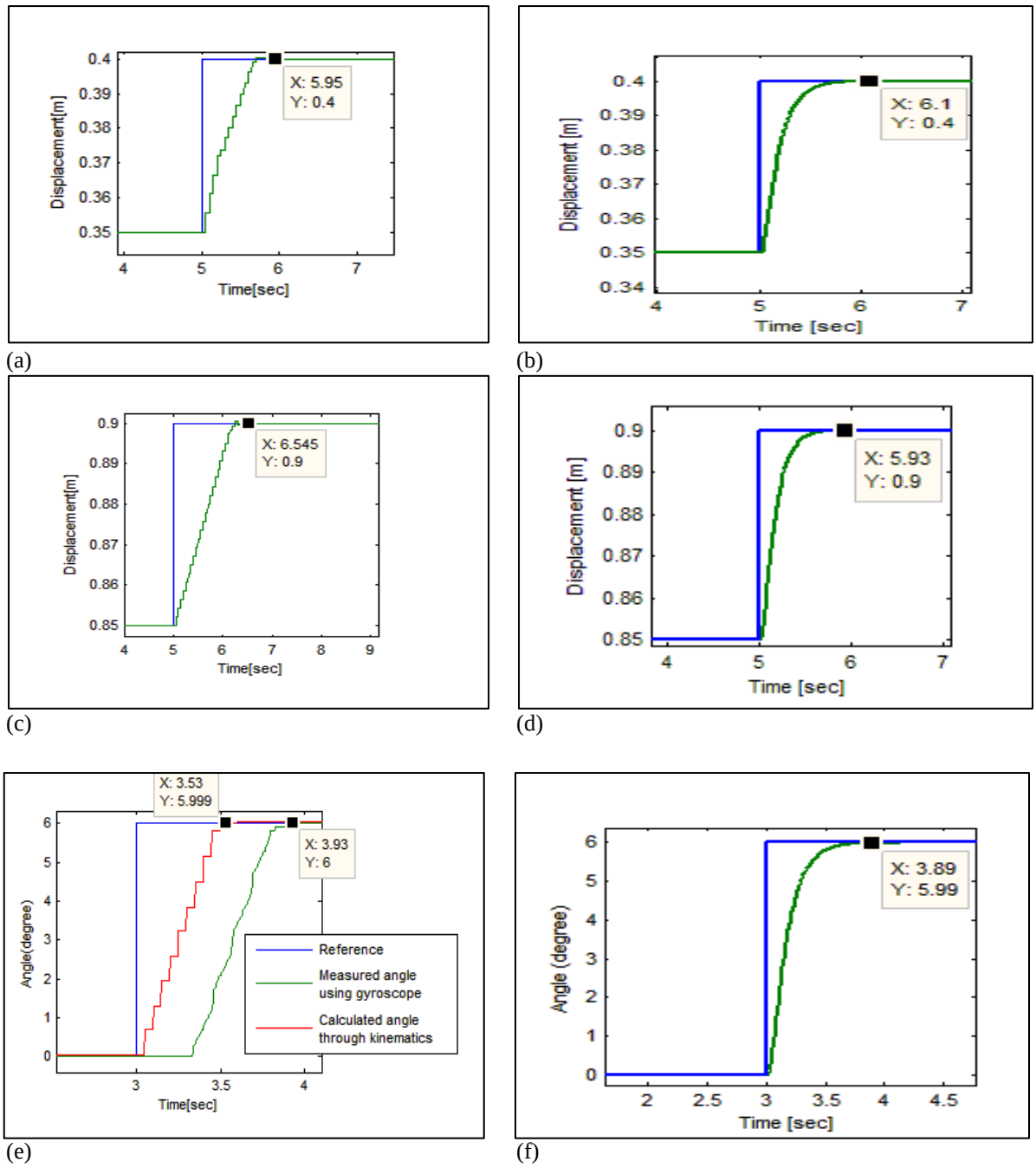

Fig. 12: Experimental results of step position input of each surge (a), heave (c), and pitch (e) using independent joint controller. In comparison with simulation results of step position input of each surge (b), heave (d), and pitch (f) using model based controller.

Discussion:

Figure 12. (a) shows the response of motion in x-direction (surge) experimentally, whereas Figure 12. (b) shows the simulation response of surge; from the results, experimental response is pretty adequate of steady state error of 0.05 and settling time 13% faster than experiment. While as the set of heave position experimentally of zero steady state error and settling time 66% slower than experiment, and both with no overshoot.

For pitch motion two ways are considered to calculate the position, the first one is through the kinematics of 0.001 steady state error and settling time of 40% faster, the gyroscope based calculation has delay time observed, due to instruments delay.

More accurate findings can be extracted with taking into consideration mass of connecting links and actuators, and friction of joints throughout dynamic model.

While independent joint controller shows good results compared to model based controller, it's reliability is a concern subject when moving platform with relatively high speed. Available linear motors used in the prototype were limited when it came to speed. Each had a maximum speed of 3 $[cm/sec]$, so results were taken with maximum speed considered. For applying model based controller on the prototype, forces are to be applied upon each joint. For available motors could not provide demanded changing forces, independent joint controller was considered.

While simulating, standing on object is assumed to be on vertical coincidence with platform center at all times which is demonstrated through dynamic model. Applying disturbance from the actual model of standing on subject will give more accurate results.

Model based controller is tested in MATLAB Simulink software environment, where plant is replaced with nonlinear model of the platform, using S function tool.

Conclusion:

A novel design of Stewart platform of particular motions of surge, heave, and pitch was proposed in this paper. Several key elements were demonstrated including overall design, structural analysis, kinematics, dynamics, and controller design, also simulation, and experimental results of platform in motion were shown, where MATLAB Simulink were used to acquire those result.

Platform was designed for the purpose of testing humanoids postural capabilities in sagittal plane, thus motions of surge, heave, and pitch were the output of the novel suggested design. While the introduced design provides three kinds of motions, a future work could be done so the platform can provide 4^{th} motion of tilting side by side (rolling). Also model could be worked upon to describe friction of joints and actuating joints which were not considered in the provided dynamic model.

REFERENCES

Tahboub, K.A., 2011. 'Biologically-inspired postural and reaching control of a multi-segment humanoid robot', Int. J. Biomechatronics and Biomedical Robotics, 1(3): 175-190. Biographical

Takashi Harada and Podi Liu, 2013. "Internal and External Forces Measurement of Planar 3-DOF Redundantly Actuated Parallel Mechanism by Axial Force Sensors," ISRN Robotics,Article ID 593606, 8 pages, 2013. doi:10.5402/2013/593606.

Brecht, Derek K., 2015. "A 3-DOF Stewart Platform for Trenchless Pipeline Rehabilitation". Electronic Thesis and Dissertation Repository. pp: 3156.

Philip J. Houdek, 1990. "Design and Implementation Issues for Stewart Platform Configuration Machine Tools." B.S., Mechanical Engineering, Boston University.

Spong, M. and M. Vidyasagar, 1989. Robot Dynamics and Control, Wiley, New York.

Ştefan STAICU "Dynamic Analysis of the 3-3 Stewart Platform" UPB Scientific Bulletin, Series D: Mechanical Engineering 71(2): 3-18.